Parametric Study of Active Solar Heating Using a Pebble Bed as a Thermal Collector and Storage Unit

Saad Mohsen Saleh
Assistant Professor
College of Engineering-University of Baghdad
E-mail: almashatsaad@yahoo.com

Mustafa Mahdi Mustafa Alaskari
Assistant Lecturer
College of Engineering-University of Baghdad
E-mail: mustafa1eng@gmail.com

ABSTRACT

In this study, pebble bed as an absorber and storage material was placed in a south facing, flat plate air-type solar collector at fixed tilt angle of (45°). The effect of this material and different parameters on collector efficiency has been investigated experimentally and theoretically. Two operation modes were employed to study the performance of the solar air heater. An integrated mode of continuous operation of the system during the period of (11:00 am – 3:00 pm) and non-integrated mode in which the system stored the solar energy through the day then used the stored energy during the period of (3:00 pm – 8:00 pm). The results of parametric study in case of continuous operating showed that the maximum average temperature difference of air between inlet and outlet sections observed on (0.018 kg/s) air mass flow rate were exceeded (17°C) and the maximum outlet temperature that got was exceeded (34°C) for the three months (December, January and February) of experiments. Average efficiency was ranged from 53% to 65%. In the case of storage and then operating, the maximum outlet air temperature was ranged from (27°C) up to (31°C) then decreased with spend of energy to reach (13°C) to (18°C) and the maximum storage energy was (165.14 W) for the porosity of (0.29) , height of (20 cm) and (0.01 kg/s) mass flow rate. The results also, showed that the solar air collector supplied a solar heating fraction (SHF) with an average of (0.65) for a meeting room (3 * 4 * 7 m) located in Baghdad as a case study.

Keywords: pebble bed, active solar heating, thermal collector and storage, experimental and theoretical study

دراسة استدلالية للطاقة الشمسية الفعالة باستخدام فرشة الحصاة كوحدة جمع وخزن للحرارة

سعد محسن صالح
استاذ مساعد
كلية الهندسة / جامعة بغداد

مصطفى مهدي مصطفى العسكري
مدرس مساعد
كلية الهندسة / جامعة بغداد

الخلاصة

في هذه الدراسة، وضعت فرشة حصاة باعتبارها مادة امتصاص وتخزين للحرارة باتجاه الجنوب ، وقد تم اجراء دراسة عملية ونظرية لاداء المجمع الشمسي بزاوية مائلة ثابتة (45°) ودراسة تغيير العوامل المختلفة على كفاءة المجمع الشمسي. تم تشغيل المنظومة بطريقتين للتشغيل لتقييم اداء منظومة تجميع الطاقة الشمسية. طريقة متكاملة من التشغيل المستمر للمنظومة الشمسية خلال الفترة (11:00 am – 3:00 pm) و طريقة غير متكاملة حيث يتم خزن الطاقة الشمسية خلال النهار و تستخدم الطاقة الشمسية المخزونة لاحقا خلال الفترة (3:00 pm – 8:00 pm). أظهرت نتائج الدراسة في حالة التشغيل المستمر أن معدل الحد الأقصى للفرق في درجة حرارة دخول و خروج الهواء من المجمع الشمسي كانت عند معدل تدفق (0.018 kg/s) والتي تجاوزت (17°C) واعلى درجة حرارة للهواء الخارج من المجمع الشمسي تجاوزت (34°C) لفترة الثلاثة أشهر (ديسمبر، يناير وفبراير) من التجارب. وقد تراوحت متوسط كفاءة المجمع الشمسي من 53% إلى 65%. اما في حالة التخزين والتشغيل، تراوحت درجة الحرارة القصوى لمخرج الهواء من المجمع الشمسي من (27°C) الى (31°C) ثم انخفضت مع

استهلاك الطاقة ليصل الى مدى تراوح من (13˚C) إلى (18˚C). وكانت طاقة الخزن القصوى (165.14 W) وذلك عندما كانت المسامية (0.29) و ارتفاع فرشة الحصاة (20 cm) وبمعدل تدفق للهواء (0.01kg/s). أيضا، أظهرت النتائج أن المجمع الشمسي الهوائي يجهز نسبة تدفئة بالطاقة الشمسية (SHF) بمتوسط (0.65) لغرفة الاجتماعات الواقعة في بغداد كحالة دراسية.

الكلمات الرئيسية: فرشة الحصاة, التدفئة الشمسية النشطة, التجميع والخزن الحراري, دراسة عملية ونظرية

1. INTRODUCTION

It is becoming increasingly necessary for countries to obtain power from sources other than conventional fossil fuels. This is as a consequence of an increasing population, people becoming more aware of environmental constraints, and the rising cost of conventional fuels. Nuclear and renewable energy sources will have to provide an increasing percentage of total power capacity. Nuclear power is still reliant on limited sources of fuel, and has strong environmental and political implications, limitations by which renewable energy is generally unaffected. It therefore makes sense to consider renewable energy sources as a means of power generation. The largest supply of renewable energy is in the form of solar energy. Several improvements have been suggested in literature to enhance the performance of the system. The use of porous material inside the collector is one method to enhance solar air heater efficiency as suggested by , **Donald** and **John, 1983**. , **Paul** and **Saini, 2003**, **Mittal et al., 2005** and **Ahmed** and **Mohamad, 2007**. Theoretical and experimental study for a solar collector was presented by **Murshid, 2005**. Using porous medium as storage material and heating source, the solar collector was made in case of continuous operating from 9:00 AM to 4:00 PM. The maximum difference between air input temperature and air output temperature from solar collector was reached (15°C) and the maximum efficiency of the solar collector reached up to (50%). Different porous materials have been suggested, such as mild steel particles, **Yeong, 2011**. Fused silica glass, alumina and stainless steel were used by **Mawire, 2009**. **Degirmencioglu, 2006**, investigated the effect of the open-cell polyurethane foam as an absorber material, placed in a south facing, flat plate air-type solar collector at fixed tilt angle on collector efficiency, Collector is tested under the regulations of ASHRAE 93-1986 standard named “Methods of Testing to Determine the Thermal Performance of Solar Collectors”. Air passing through the collector has been provided by a fan. Tests are repeated with three air speeds 1.266 m/s, 1.5825 m/s and 1.899 m/s. Maximum average efficiency is calculated on 1.5825 m/s. Maximum average temperature difference of air between inlet and outlet sections observed on 1.266 m/s. Maximum outlet temperature that we get is on the same day with maximum average temperature difference. , **Mohanraj** and **Chandrasekar 2009**, developed and tested performance of an indirect forced convection solar drier integrated with different sensible heat storage maternal. The system consists of a flat plate solar air heater with heat storage unit, a drying chamber and a centrifugal blower. Drying experiments have been performed at an air flow rate of 0.25 kg/s. Drying of chili in a forced convection solar drier reduces the moisture content from around 72.8% (wet basis) to the final moisture content about 9.1% in 24 h. Average drier efficiency was estimated to be about 21%. The specific moisture extraction rate was estimated to be about 0.87 kg/kWh.

In this study, the advantage of using packed beds of pebble to store thermal energy for solar collector has been determined. Effects of various parameters (porosity, height of pebble bed and mass flow rate) on the collector performance had also been investigated.

2. MATHEMATICAL MODEL

The packed bed solar air heater model has been considered for this present study is shown in **Fig 1.** The collector consists of a glass cover plate, a blackened absorber plate and a back plate with blackened pebbles packed in the airflow passage between the absorber and the black colored back plate.

The MATLAB program is used in this work for computer programming. The computation is composed of a main program for one day per month of experiment work. Also it is applicable for each day of the experiment work by changing the variable inputs and the condition of experiment day.

Simplified steps were used to analyze the heat transfer for the air flow across the pebble bed and to calculate the amount of energies and the efficiency. The calculations were based on the following assumptions: (a) study state. (b) one dimensional heat transfer across the glass cover. (c) constant temperature across thickness of glass cover. (d) one dimensional heat transfer across insulation layers. (e) one dimensional heat transfer across the porous media.

2.1 Absorption Energy Calculation

The absorption energy could be calculated by the equation below:

$$Q_{ab} = F_t * I_t * A \tag{1}$$

F_t is calculated from Eq. (2) as:

$$F_t = (\alpha_p \tau_g)_e * F_{sh} * F_d \tag{2}$$

2.2 Loss Energy Calculation

Losing energy is happening from all sides of the solar collector, in spite of the biggest part of losing is from the absorber surface. However, losing energy from sides and bottom has a clear effect.

The amount of losing energy is given by the following equation:

$$Q_{loss} = U_l * A * (T_p - T_a) \tag{3}$$

Mean plate temperature (T_p) is calculated by **Duffie** and **Beckman, 2008**, as follows:

$$T_p = T_i + \frac{Q_u/A}{F_R U_l}(1 - F_R) \tag{4}$$

The collector overall heat transfer coefficient (U_l) is the sum of top, bottom and edge loss coefficients:

$$U_l = U_t + U_b + U_e \tag{5}$$

The top loss coefficient from the collector plate to the ambient for this single glass cover system is as follows:

$$U_t = \left[\frac{1}{h_{c,p-g} + h_{r,p-g}} + \frac{1}{h_w + h_{r,g-a}}\right]^{-1} \tag{6}$$

The wind heat transfer coefficient is calculated as **Duffie** and **Beckman, 2008**.

$$h_w = 5.7 + 3.8\, v \tag{7}$$

The radiation heat transfer coefficient from the glass to the air ($h_{r,g-a}$) is calculated as:

$$h_{r,g-a} = \varepsilon_g \sigma (T_g + T_s)(T_g^2 + T_s^2) \qquad (8)$$

The radiation heat transfer coefficient from the plate to the glass cover ($h_{r,p-g}$) is calculated as:

$$h_{r,p-g} = \frac{\sigma (T_p + T_g)(T_p^2 + T_g^2)}{\frac{1}{\varepsilon_p} + \frac{1}{\varepsilon_g} - 1} \qquad (9)$$

The convective heat transfer coefficient is calculated as:

$$h_{c,p-g} = \frac{Nu\, K}{D_h} \qquad (10)$$

where $D_h = p_t \frac{2Wd}{W+d}$, (P_t= porosity).

Nusselt number Nu is a function of Rayleigh number *Ra* which is given by , **Duffie** and **Beckman, 2008**.

$$Nu = 1 + 1.44\, [1 - \frac{1708\, (\sin 1.8\beta)^{1.6}}{Ra \cos\beta}][1 - \frac{1708}{Ra \cos\beta}]^{+} + [(\frac{Ra \cos\beta}{5830})^{\frac{1}{3}} - 1]^{+} \qquad (11)$$

The heat removal factor F_R is given as:

$$F_R = F'' F' \qquad (12)$$

Where the collector flow factor F'' and the collector efficiency factor F' are calculated as follows:

$$F'' = \frac{\dot{m}_a c_p}{A U_l F'} [1 - \exp(-\frac{A U_l F'}{\dot{m}_a c_p})] \qquad (13)$$

$$F' = [1 + \frac{U_l}{h + (\frac{1}{h} + \frac{1}{h_r})^{-1}}]^{-1} \qquad (14)$$

The radiation coefficient between the two air duct surfaces at a mean fluid temperature T_{mf} is:

$$h_r = \frac{4\, \sigma\, T_{mf}^3}{\frac{1}{\varepsilon_p} + \frac{1}{\varepsilon_g} - 1} \qquad (15)$$

The heat transfer coefficient inside the duct is:

$$h = Nu1 \frac{K}{D_h} \qquad (16)$$

Where $Nu1 = 0.0158\, Re^{0.8}$

The useful gain is calculated as follow:

$$Q_u = F_R A [S - U_l (T_i - T_a)] \qquad (17)$$

Which is also can be calculated as:

$$Q_u = \dot{m}_a * c_p * (T_o - T_i) \quad (18)$$

"eq. (16) dependent in experimental calculation"

From Eq. (17) & (18), the outlet temperature is:

$$T_o = T_i + Q_u/\dot{m}_a * c_p \quad (19)$$

2.3 Thermal Efficiency Calculation

The efficiency of the flat-plate solar collector (η_c) is defined as the ratio of the rate of useful energy supplied by the collector (Q_u) to the rate of incident solar energy in its area.

$$\eta_c = \frac{Q_u}{Q_I} \quad (20)$$

2.4 The Performance of a Solar Collector in an Active System

It's a simple procedure which has been devised by **Balcomb** and **McFarland, 1978** and used by the researcher **Murshid, 2005** for predicting the performance of solar collector in active systems. This calculation can be made based on the values of solar radiation, heating degree days, and the thermal loss and solar gain characteristics of the building. In this study, load collector ratio (LCR) was used as the following steps.

Estimate the building loss coefficient (BLC). This is the sum of the building skin conductance plus infiltration.

$$BLC = (\sum UA_s + INF) * 24 * 3600 \quad (21)$$

The solar heating fraction (SHF) is the fraction of save energy to the net load which is calculated as follows:

$$SHF = Q_{save} / Q_{net} \quad (22)$$

$$Q_{save} = \dot{m}_a * c_p * \sum_1^{24} (T_{ao} - 18)^+ \quad (23)$$

$$Q_{net} = BLC * DD \quad (24)$$

$$DD = \sum_1^{24} (20 - T_a)^+ \quad (25)$$

"The (+) sign in Eqs. (23) and (25) indicate that only the positive value taken into account"

The auxiliary energy (Q_{aux}) required keeping the building at (20°C) calculated as follows:

$$Q_{aux} = (1 - SHF) * BLC * DD \quad (26)$$

2.4 Energy Balance

Based on the assumptions that have been mentioned and used to solve mathematical equations relating to the performance of solar collector for the collection and storage, we have developed a mathematical model by performing an energy balance on the solar collector.

The equation of thermal energy balance is written as shown in **Fig. 2**

(Energy absorbed by the surface absorber) + (Energy entering the air solar collector) = (Energy leaving the air solar collector) + (Stored Energy) + (Energy lost from the solar collector)

This can be written in the formula as follows:

$$I_t * A + \dot{m}_a * c_p * T_i = \dot{m}_a * c_p * T_o + E_{st} + U_l * A * (T_p - T_a) \quad (27)$$

The above equation can be written as:-

$$Q_{st} = I_t * A - \dot{m}_a * c_p * (T_o - T_i) - U_l * A * (T_p - T_a) \quad (28)$$

3. EXPERIMENTAL WORK

Air-type solar collector was used in this project. Basically the experimental setup consists of three main mechanical parts. First and the most important part is the collector itself. Second part is the inlet and outlet channels. Third part is the blower that provides air stream during experiments. Pebble bed with (0.29) and (0.34) porosity placed in the collector flow channel in order to increase heat transfer area.

The solar collector is made locally for the purposes of collect and storage at the same time. It consists of a reservoir of iron with dimensions of (1x0.6x0.25 m) and a thickness of (2 mm) for the purpose of carrying the weight of the porous material used to make the tank in case of consistency and stability. Three brackets of iron mesh were installed to support and facilitate the development of porous media in the collector reservoir, and also to distribute air evenly across the porous media. (1mm) thickness aluminum plate was used as absorber plate and coated with black color to receive maximum amount of solar incident radiation. The solar collector was isolated from all sides and bottom with class wool insulation of (5cm) thickness to reduce the heat losses. A glass cover (4mm) thickness and (1x0.6m) dimensions applied at the surface of the solar collector. It was sealed to prevent leakage of water into the solar collector or heat air loss. The gap between the glass cover and the absorber plate was ranged from (5cm) when the pebble bed depth was (20cm), and it was (10 cm) when the pebble bed depth was (15cm).

The experiments were conducted on the days of December, January and February in Baghdad. The collector was located with 45 angle towards the south (For winter load, the tilt should be (latitude + 10) degrees and for year round use, the tilt = latitude, [12]). **Fig. (1)** shows the general aspect of experimental setup. The experiments were carried out at the same time periods between (11:00 to 15:00) of the days (In the case of continuous operation) and between (15:00 to 20:00) of the days (In the case of storage and operation) for (0.01 kg/s) & (0.018 kg/s) of mass flow rates. The air flow through the collector was supplied by an electric blower and adjusted via a regulator integrated with the blower. The velocity of the air was measured by an anemometer sensor. The incident solar radiation on collectors' inclined upper surface was measured up to date by (Datalogging Solar Power Meter TES-1333R). Type K thermocouples were placed at inlet, outlet flow channels, back plate, pebble bed, absorber plate, glazing cover of the collector and a free one to measure ambient temperature.

4. RESULTS AND DISSCUSION

Fig. 3 shows the variation of the intensity of solar radiation with time for the days (21 Dec., 5 Jan. and 10 Feb.). As shown in this figure, the intensity of solar radiation increases steadily with time and attained peak values at the mid-day then decrease steadily with time as the sun goes down in the late afternoon. It observed that the maximum solar intensity reaches to (764.5 W/m^2) in (21 Dec) and it is reached to (1005 W/m^2) in (5 Jan) while it is (900.3 W/m^2) in (10 Dec).

In the case of continuous operating for the solar collector the solar collector has been run with electric blower which is working from 11:00 am to 3:00 pm. The temperature was measured at different sections, air inlet, air outlet, back plate, pebble bed, absorber plate, glazing cover of the collector and the ambient. According to these measurements, the efficiency, the useful, storage and loss energy were calculated. **Fig. 4** shows the effect of height of the pebble bed on average temperature (by using thermocouples distributed at three equal distance) of porous media with time for mass flow rate of (0.01 kg/s) for days in Dec., Jan. and Feb. The temperatures of porous media increase gradually from (11:00 am) and reach the maximum value at (3:00 pm) which exceed (30°C) with height of (15 cm) of pebble bed. In one hand variation of temperature of the porous media with time because the intensity of solar radiation increase gradually and through this period the temperature of absorber plate increase and this is lead to increase of the temperature of porous media. In another hand it can be observed that the maximum temperature of pebble bed is at (15 cm) because it heated faster than (20 cm) pebble bed height.

Fig. 5 shows the variation of inlet air temperature to the collector and the experimental and theoretical outlet air temperature with time for (0.018 kg/s) mass flow rate for the days of (21 Dec., 5 Jan. and 10 Feb.). **Fig. 5a** shows a convergence between the experimental and theoretical outlet air temperature and matching point at 12:30 pm. The maximum outlet air temperature from the solar air collector was (35.5°C experimentally and 33.07°C theoretically). The maximum temperature difference between inlet and outlet air from the solar collector was (17.9°C). The convergence with less error was found in **Fig. 5b** and the matching was achieved from (1:00 to 2:00 pm). The maximum outlet air temperature from the solar air collector was (34.6°C experimentally and 33.03°C theoretically) and the maximum temperature difference between inlet and outlet air from the solar collector was (20°C). The same behavior was shown in Fig. (5c) with matching points at (1:00 and 1:30 pm) respectively. The maximum outlet air temperature from the solar air collector was (34.3°C experimentally and 32.9°C theoretically) and the maximum temperature difference between inlet and outlet air from the solar collector was (18.2°C). The differences between the experimental and theoretical values in the previous figures because of the different in the theoretical values of useful energy which are actively involved in the Eq. (19), and that because the theoretical calculation of solar intensity which effect on useful energy are different from the experimental values of solar intensity. The average of the maximum outlet air temperature from the solar air collector was (34.8°C) and the average of the maximum temperature difference between inlet and outlet air from the solar collector was (18.7°C).

Fig. 6 shows the variation of thermal efficiency with solar radiation for mass flow rate of (0.01 and 0.018 kg/s) respectively, pebble bed height of (15 cm) and (0.34) porosity for the days of (22 Jan. and 2 Feb.). The efficiency increases with an increase in the solar radiation. This is due to the increase of temperature difference which is directly proportion to the efficiency. But it can be seen that even when the solar radiation decrease after (1:30 pm), the efficiency continue to rise. This is also because increase of temperature difference and this is a positive point for use the porous media that help to store heat even when the sun goes down in the late afternoon.

The effect of temperature rise on the efficiency of the solar collector for mass flow rate of (0.01 and 0.018 kg/s), pebble bed height of (15 cm) and (0.34) porosity for the days of (22 Jan. and 2 Feb.) is shown **Fig. 7.** The thermal efficiency increases with the increase in the temperature rise because of the direct proportion of efficiency with the temperature rise that has direct proportion to the useful gain and that approved by applying Eq. (20).

The effect of mass flow rate of air on the variation of inlet and outlet air temperature difference with time is shown in **Fig. 8** for different height and porosity of the pebble bed. It has been observed that the temperature difference increases with increase in mass flow up to (26%). The figure also shows that the temperature difference has been reached the maximum value between (1:30 to 2:00 pm) then the curve goes down for the days of experimental work. This is because of the behavior of solar radiation shown in **Fig. 4**. Temperature difference is directly proportion to solar radiation.

There is a significant effect of mass flow rate on efficiency. It is evident from **Fig. 9**, that for higher mass flow rate, efficiency is much higher with a rate ranging from (48%) to (54%). This behavior has been obtained experimentally and it can be approved theoretically from Eq. (20).

Fig. 10 shows the effect of porosity of pebble bed on the variation of air temperature difference between inlet and outlet of the solar collector with time, which is higher for low porosity. It has been observed that the values in the two porosity experiment are quite close, but deviation occur with time progress. It can be concluded that there is an increment ranging from (4%) to (20%) showing the effect of porosity on the temperature difference.

There was no significant effect of porosity on efficiency with higher mass flow rate. This is shown in **Fig. 11** It has been seen randomly behavior of the curves in the previous figure because of the effect of the experimental amount of solar radiation which is involve in Eq. (20), and that because the different weather in which the experiments process.

Fig. 12 shows the effect of height of pebble bed on the variation of temperature difference with time. It has been shown that the pebble bed with (15cm) height has the higher temperature difference with a rate ranging from (5%) to (29%) in Dec. and Jan. for (0.018 kg/s) air mass flow rate and ranging from (10%) to (38%) in Feb. for (0.01 kg/s) air mass flow rate. The solar radiation takes less time to reach pebble bed with (15cm) than the pebble bed with (20cm), so the lower pebble bed will get more heat and thus the higher temperature difference.

Fig. 13 shows the variation of solar heating fraction for a different height of the pebble bed. This comparison shows that for (h=15 cm) in the months of December and January, the (SHF) was higher than that for (20 cm) with a fraction reached to (57 %). While in February, the behavior was inversed because of the different in (SHF) values which are depend on the amount of solar intensity measured experimentally. The variation of auxiliary energy that we need to add it for the days of (27 Dec., 5 Jan., and 10 Feb.) and the days of (10 Dec., 10 Jan., and 23 Feb) was shown in **Fig. 14** It was observed that in (5 Jan) it is need higher auxiliary energy reached to (21, 093 kJ) while in (17 Feb.) less energy must be adding. The maximum auxiliary energy (2,276 kJ) in (23 Feb.) and it is need (2,795 kJ) in (10 Jan) these amounts depended on the (SHF) values, where the higher value (SHF) there is less need for the auxiliary energy.

5. CONCLUSIONS

The main conclusions from the present work may be stated as follows:

- The increment of efficiency due to pebble placing can be observed easily in spite of decreasing the solar radiation.
- The solar collector supply hot air up to (29 C°) with average temperature difference of (14 C°),
- The efficiency of the solar collector increases with the increment of air velocity with a rate ranging from (48%) to (54%).
- Decreasing the pebble bed height, increasing the efficiency with a rate of (4% to 30%) and the increment of the temperature difference ranging from (10%) to (38%) for a given mass flow rate.
- The variation of air temperature difference between inlet and outlet of the solar collector with time was higher for low porosity with an increment ranging from (4%) to (20%).
- The solar collector supplied a solar heating fraction (SHF) with an average of (0.65).

REFERENCES

- Ashish K., 2009, *Mathematical Modeling of Solar Air heater with Different Geometries*, M.Sc. thesis, Thapar University.

- Bashria, A., Yousef, A. and Adam, N. M, 2007, *Analysis of single and Double Passes V-Grooves Solar Collector with and without Porous Media*. International Journal of Energy and Environment,vol.2,No.1,PP.109-114.

- Beasley, D.E. and Clark J.A., 1983, *Investigation of Rock Bed Solar Collector Cum Storage System*, International Journal of Heat and Mass transfer, vol.27, No.9, PP.1659-1669.

- Bennamoun, L. and Belhamri, A., 2008, *Study of Heat and Mass Transfer in Porous Media*, Tech Science Press, vol.4, No.4, PP. 221-230.

- Cheung, A. C.; Chiang, C. W.; Chen, M. S., 1979, *Heat Transfer in a Porous Medium Flat Plate Solar Collector*, Proceedings of the Multi-Phase Flow and Heat Transfer Symposium-Workshop, PP.16-18.

- Choudhury C., Chauhan P. M. and Garg H. P., 2008, *Economic Design of a Rock Bed Storage Device for Storing Solar Thermal*, Center for Energy Studies, Indian Institute of Technology.

- Degirmencioglu, C., 2006, *The Use of Open Cell Polyurethane Foams in Air-Type Solar Collectors as the Heat Absorbing Element*, M.Sc. Thesis, The Graduate School of Engineering and Sciences of İzmir Institute of Technology.

- Garg, Bandyo and Sharma, 1981, *Investigation of Rock Bed Solar Collector Cum storage system*, Center of energy studies, Indian Technology.

- Irfan Kurtbas and Emre Turgut, 2006, *Experimental Investigation of Solar Air Heater with Free and Fixed Fins*, International Journal of Science & Technology, vol. 1, No.1, PP.75-82.

- Kenneth Guy Allen, 2010, *Performance Characteristics of Packed Bed Thermal Energy Storage for Solar Thermal Power Plants,* M.Sc. Thesis, University of Stellenbosch.

- Klein, S. A., Beckman, W. A. and Duffie, J. A., 1975, *Design Procedure for Solar Air Heating Systems*, International Solar Energy Society, Los Angeles.

- Mawire A., 2009, *Simulated Performance of Storage Materials for Pebble Bed Thermal Energy Storage (TES) Systems*, Journal of Applied Energy.

- Mittal, M.K., Varshney, L., 2005, *Optimal Thermo Hydraulic Performance of a Wire Mesh Packed Solar Air Heater*, Solar Energy, vol.80, PP.1112-1120.

- Mohandraj M. And Chandrasekar P., 2009, *Performance of a Forced Convection Solar Drier Integrated With Gravel as Heat Storage Material for Chili Drying*, Journal of Engineering Science and Technology, vol. 4, No. 3, PP.305 – 314.

- Murshid A. M., 2005, *Performance Study of Using the Active Solar Energy for Heating by Using Porous Media*, M.Sc. Thesis, University of Tikrit.

- Navarrete, J.J., Cervantes J.G., 2008, *Energy Analysis of a Rock Bed Thermal Storage System*, International Journal of Energy, vol.5, No.1, PP.18-30.

- Paul B. and Saini J. S., 2003, *Thermohydraulic Performance of Pebble Bed Solar air Heaters*. Proceedings of the International Conference on Mechanical Engineering.

- Qenawy, A. M. and Mohamad, A. A., 2007, *Analysis of High Efficiency Solar Air Heater for Cold Climates*, 2nd Canadian Solar Buildings Conference Calgary, vol.10, No.14.

- Yeong, W., Lai, Y. and Foo J., 2011, *Improvement of a Solar Heating Panel's Thermal Efficiency*, vol.4, No.1, PP.44-55.

7. NOMENCLATURE

A = area of solar collector, m^2.
As = area of skin condition, m^2.
BLC = building loss coefficient, J/DD.
Cp = specific heat of air, J/kg.°C.
Fd = dust coefficient, dimensionless.
Fsh = shading coefficient, dimensionless.
Ft = effective transmittance-absorption factor, dimensionless.
FR = heat removal factor, dimensionless.
F' = collector efficiency factor, dimensionless.
F'' = collector flow factor, dimensionless.
Dh = hydraulic diameter, m.
DD = degree-Day, °C.
H = coefficient of heat transfer, W/m^2.K.
It = total incident radiation, W/m^2.
INF = infiltration, W/°C.
K = thermal conductivity, W/m.K.
L = length of bed, m.
m.a = mass flow rate of air, kg/s.
Nu = nusselt number, dimensionless.
Pt = porosity, dimensionless.
Q = energy, W.
Ra = rayleigh number, dimensionless.
Re = reynolds number, dimensionless.
S = absorbed solar radiation, W/m^2.
SHF = solar heating fraction, dimensionless.
T = temperature, °C.

Ub = back loss coefficient, $W/m^2.K$.
Ue = edge loss coefficient, $W/m^2.K$.
Ul = overall loss coefficient, $W/m^2.K$.
Ut = top loss coefficient, $W/m^2.K$.

GREEK SYMBOLS
α = absorptance of surface for solar radiation, dimensionless.
β = tilt angle, degree.
τ = glass transmittance, dimensionless.
Δ = difference, dimensionless.
η = efficiency, dimensionless.
ε_g = penetration of glass cover, dimensionless.
σ = bultzmann constant, dimensionless.
ε_p = emittance of surface, dimensionless.

SUBSCRIPTS
a = ambient, dimensionless.
b = bottom, dimensionless.
c = convection, dimensionless.
e = edge, dimensionless.
f = fluid, dimensionless.
g = glass, dimensionless.
i = inlet, dimensionless.
m = mean, dimensionless.
o = outlet, dimensionless.
p = plate, dimensionless.
r = radiation, dimensionless.
u = useful, dimensionless.

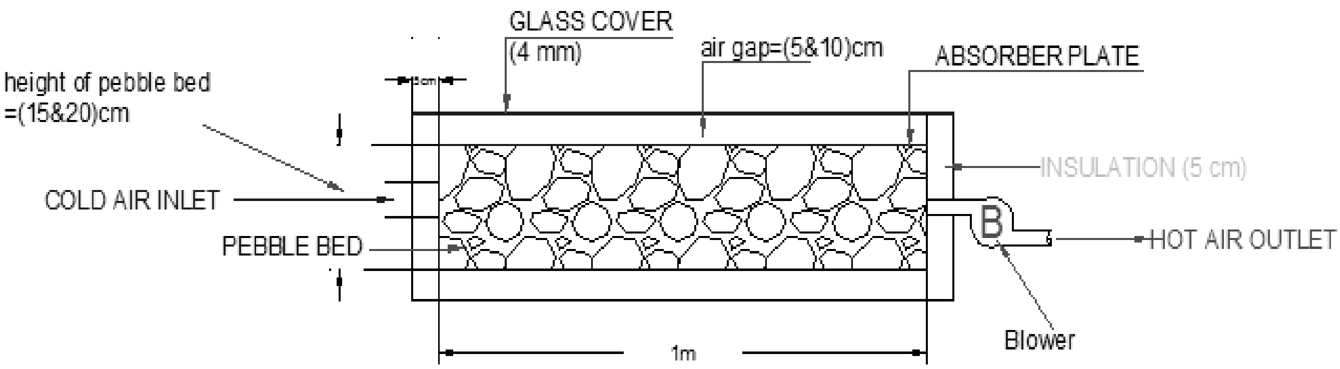

Figure 1. Cross section of the solar air heater.

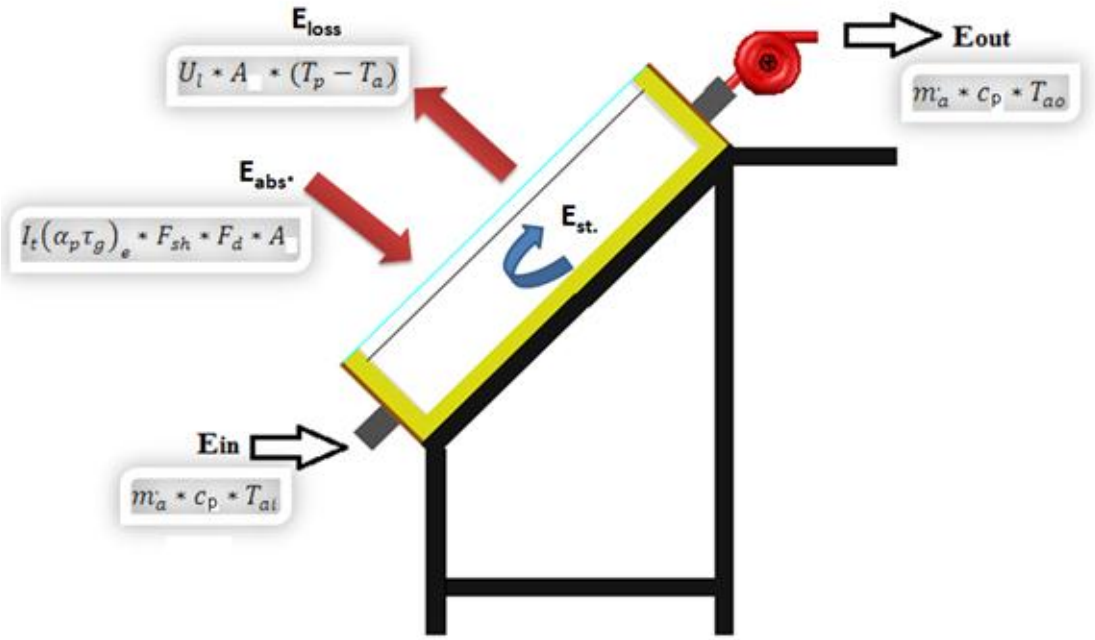

Figure 2. Energy balance on the solar collector.

Parameters: (h=height of pebble bed, m'=air mass flow rate, p=porosity)

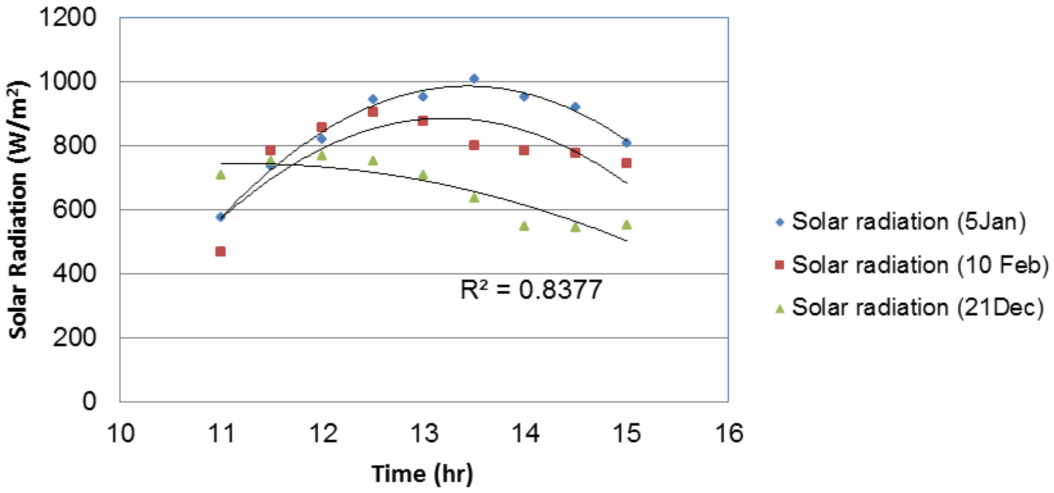

Figure 3. Variation of Solar radiation with time (h=20 cm, m'=0.018 kg/s , p=0.29).

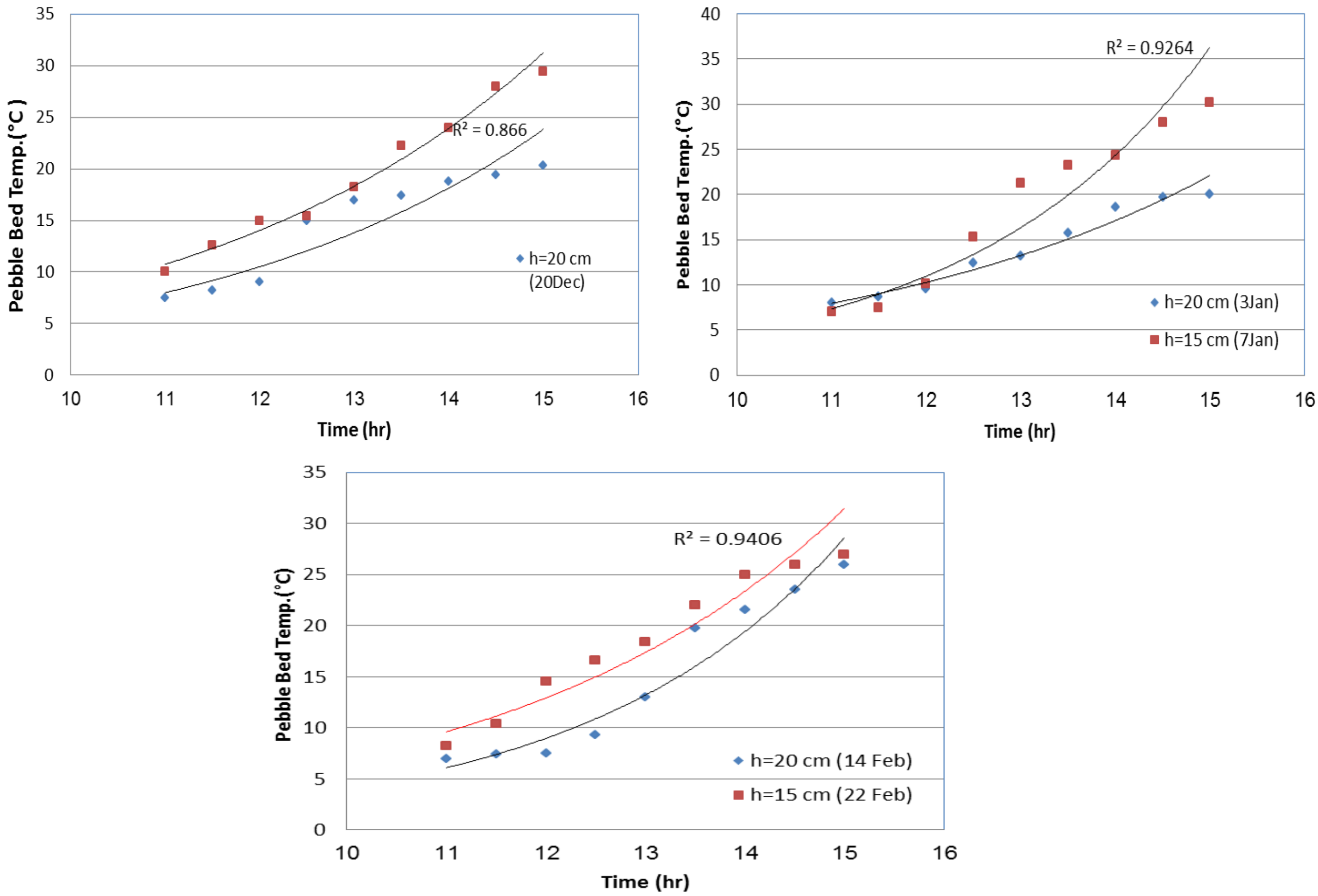

Figure 4. Variation of temperature of porous media with time for different pebbles bed heights (m'=0.01 kg/s, p=0.29).

(a)

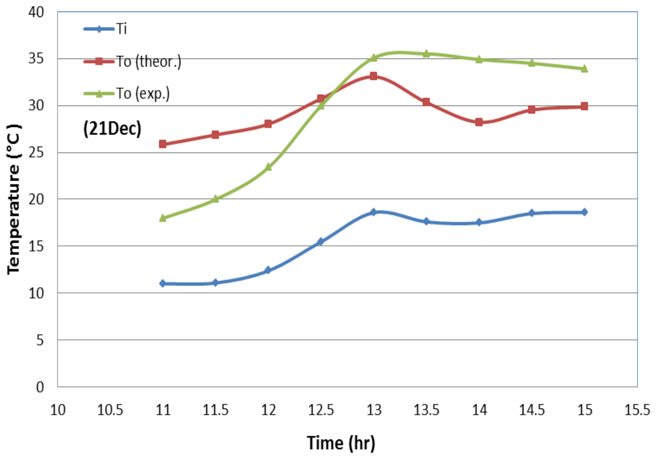

(b)

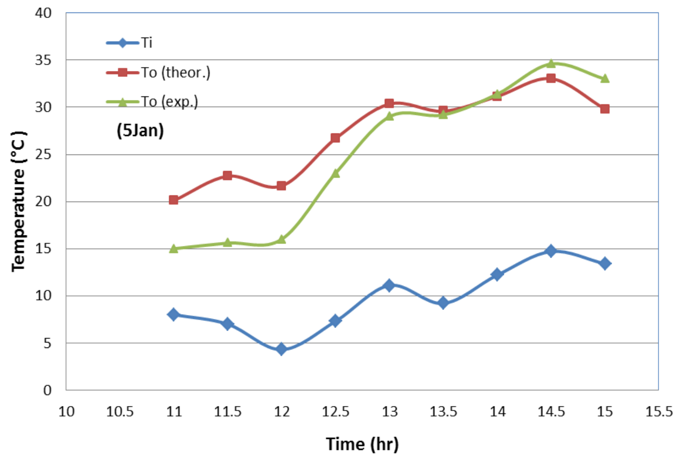

(c)

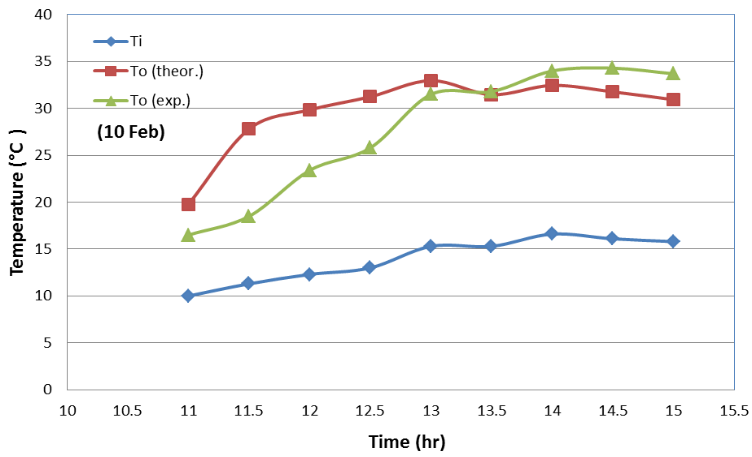

Figure 5. Variation of inlet and outlet temperatures with time (h=20 cm, m'=0.018 kg/s , p=0.34).

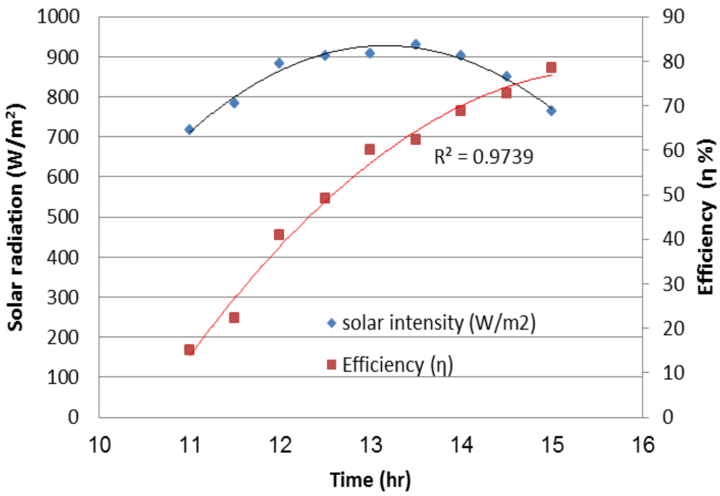

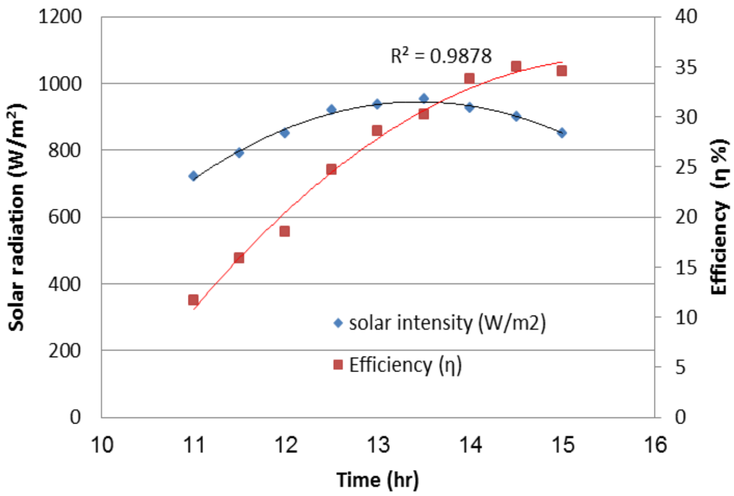

Figure 6. Effect of solar radiation on efficiency with time.

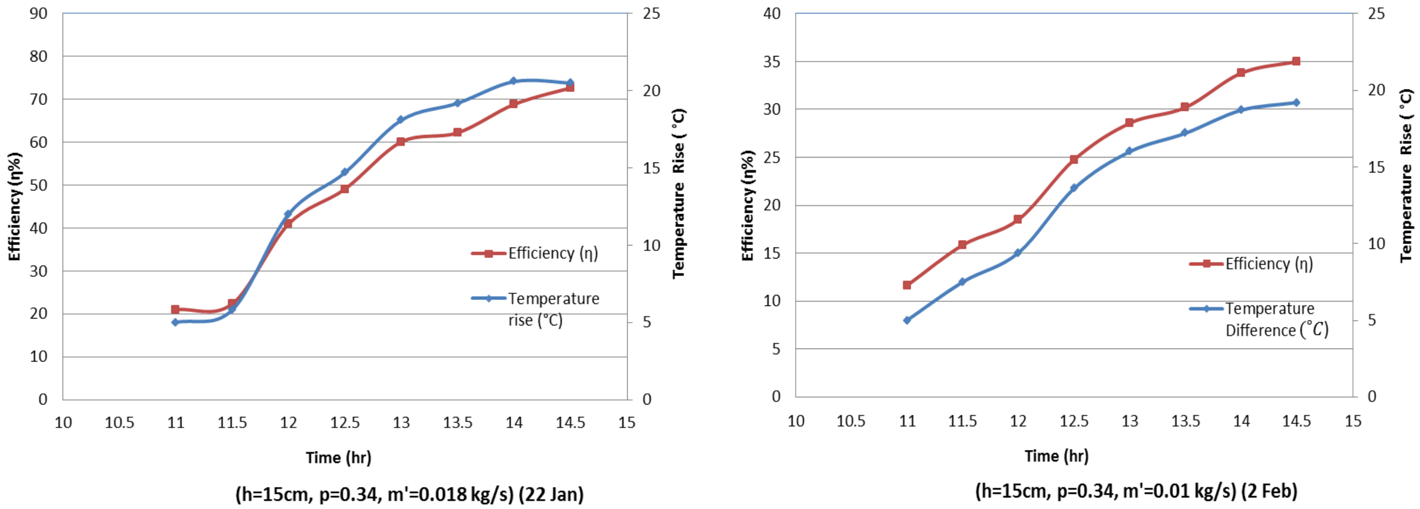

Figure 7. Effect of temperature rise on efficiency with time.

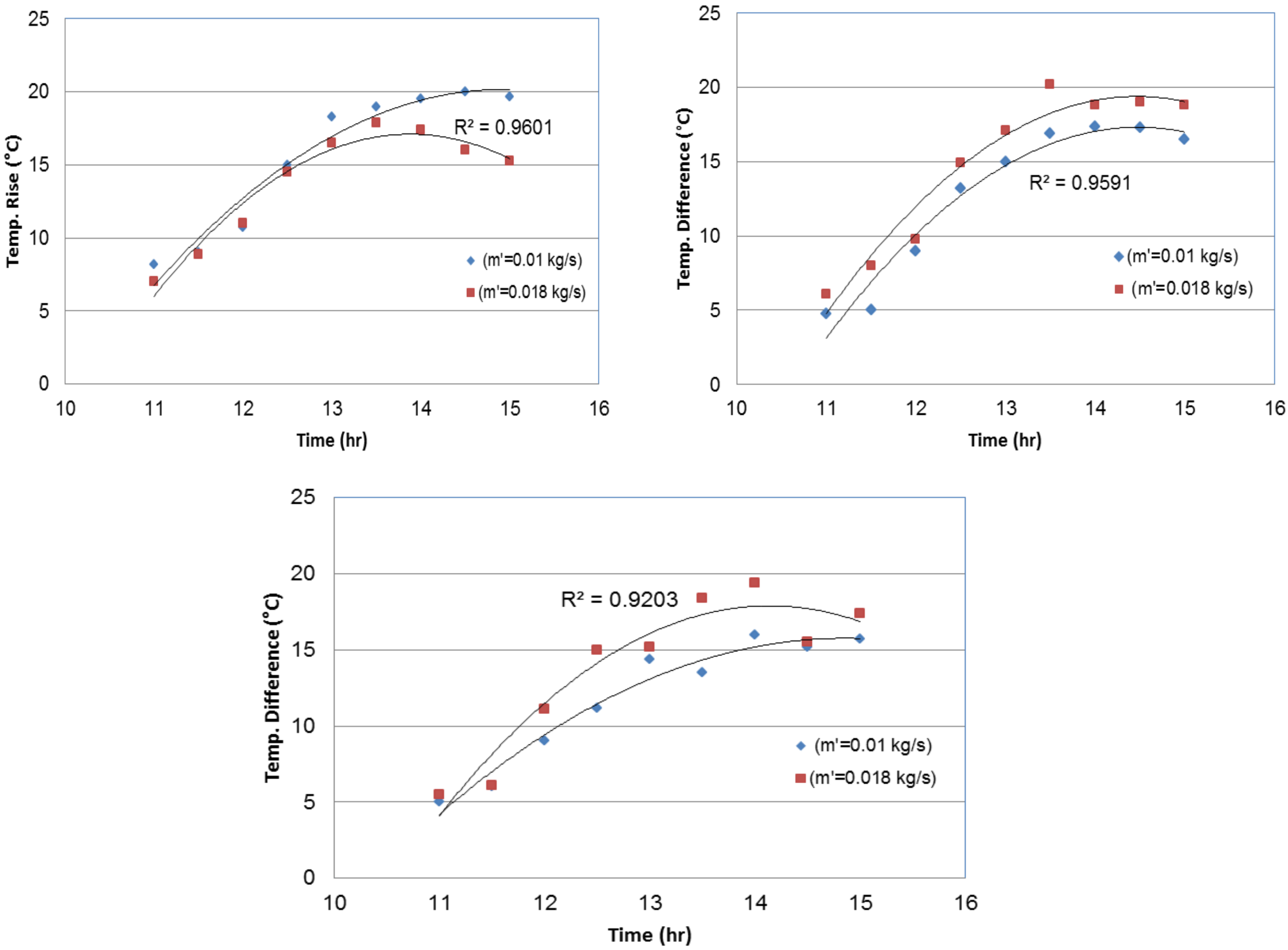

Figure 8. Effect of mass flow rate on variation of temperature rise with time.

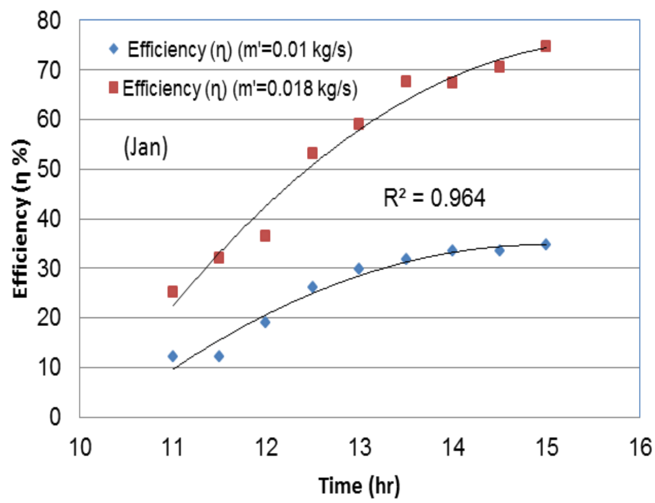

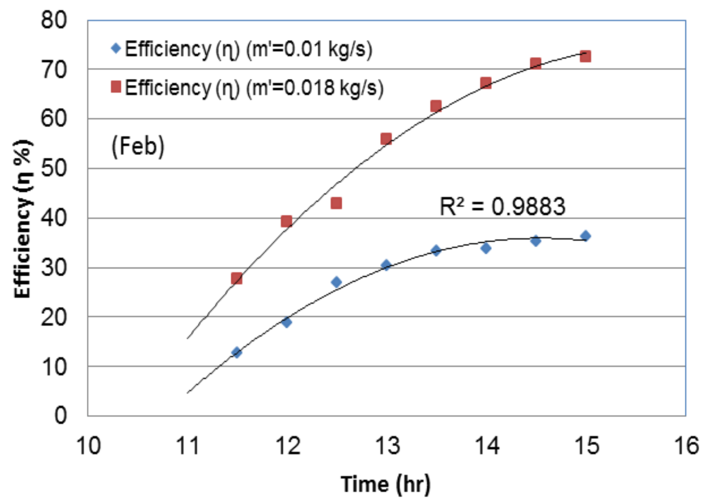

Figure 9. Effect of mass flow rate on variation of efficiency with time.

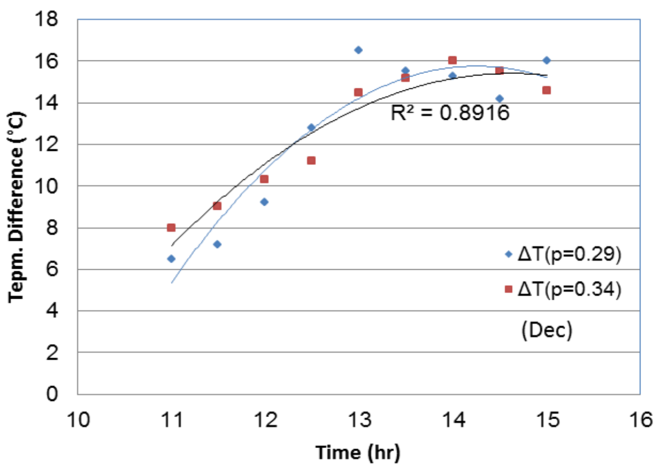

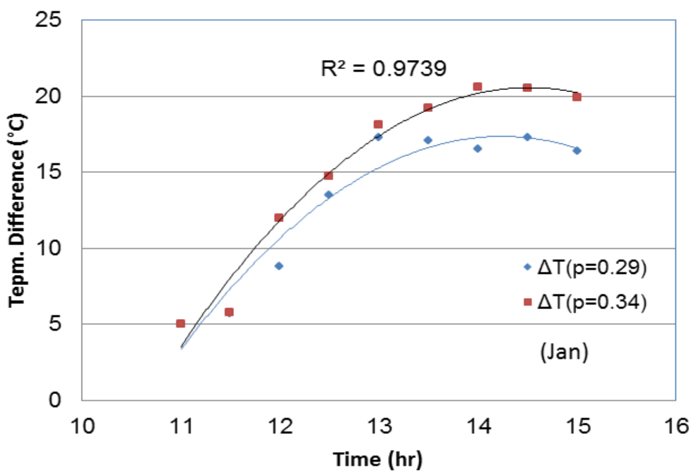

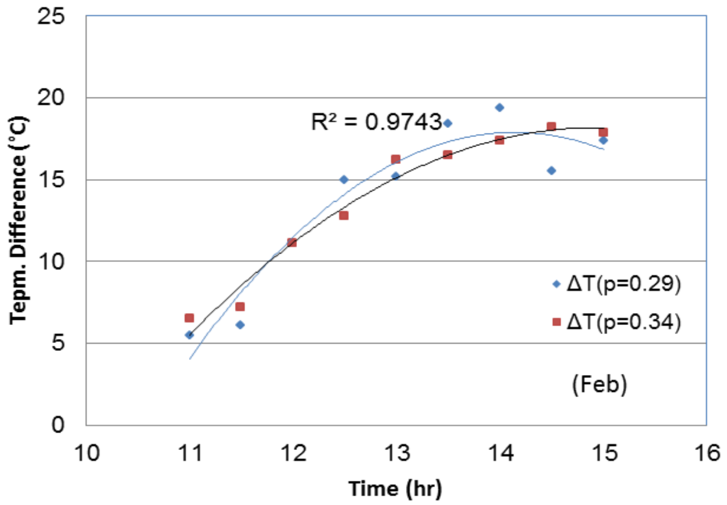

Figure 10. Effect of porosity on va

(h=20 cr

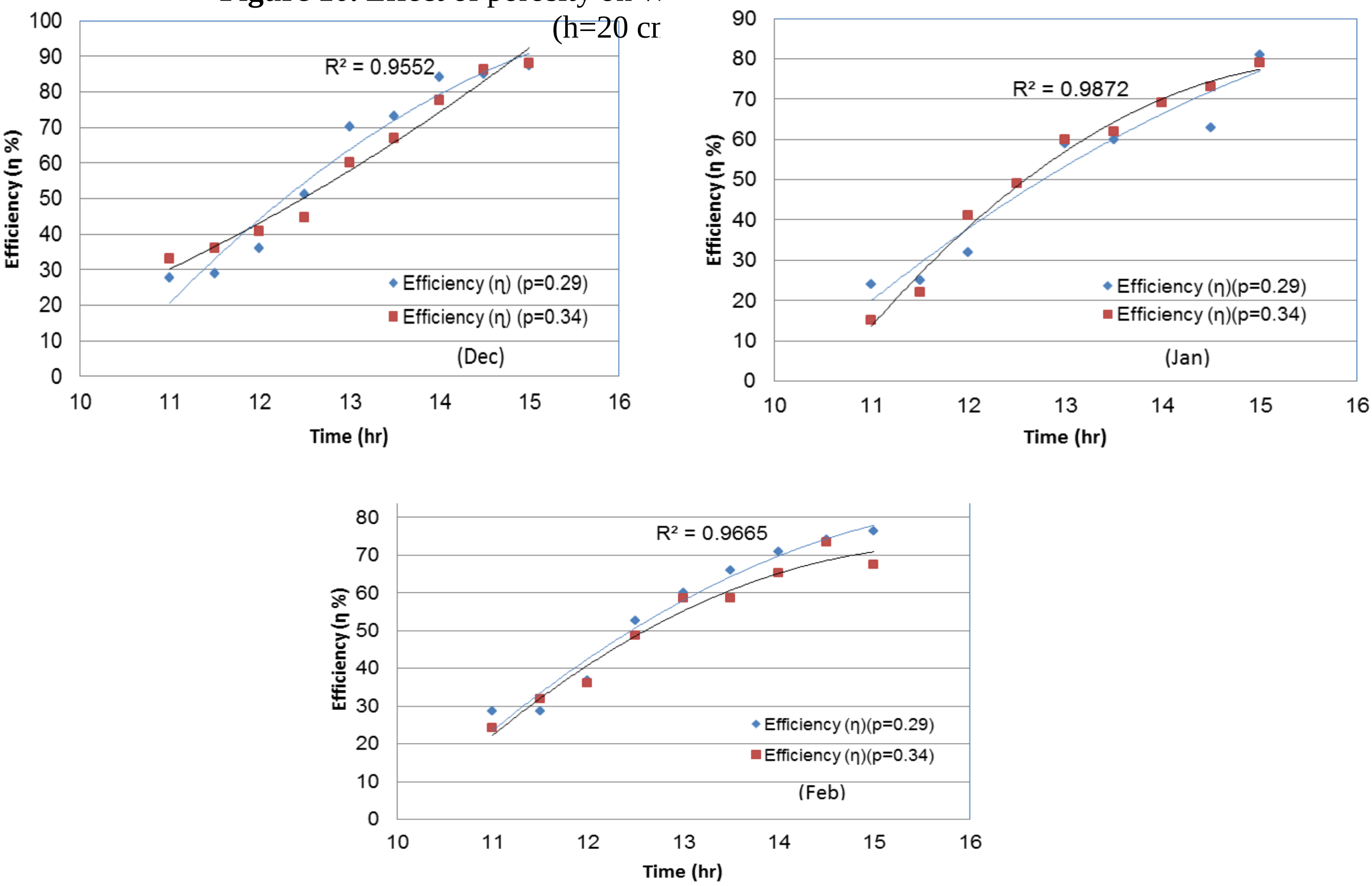

Figure 11. Effect of porosity on variation of efficiency with time (h=15 cm, m'=0.018 kg/s).

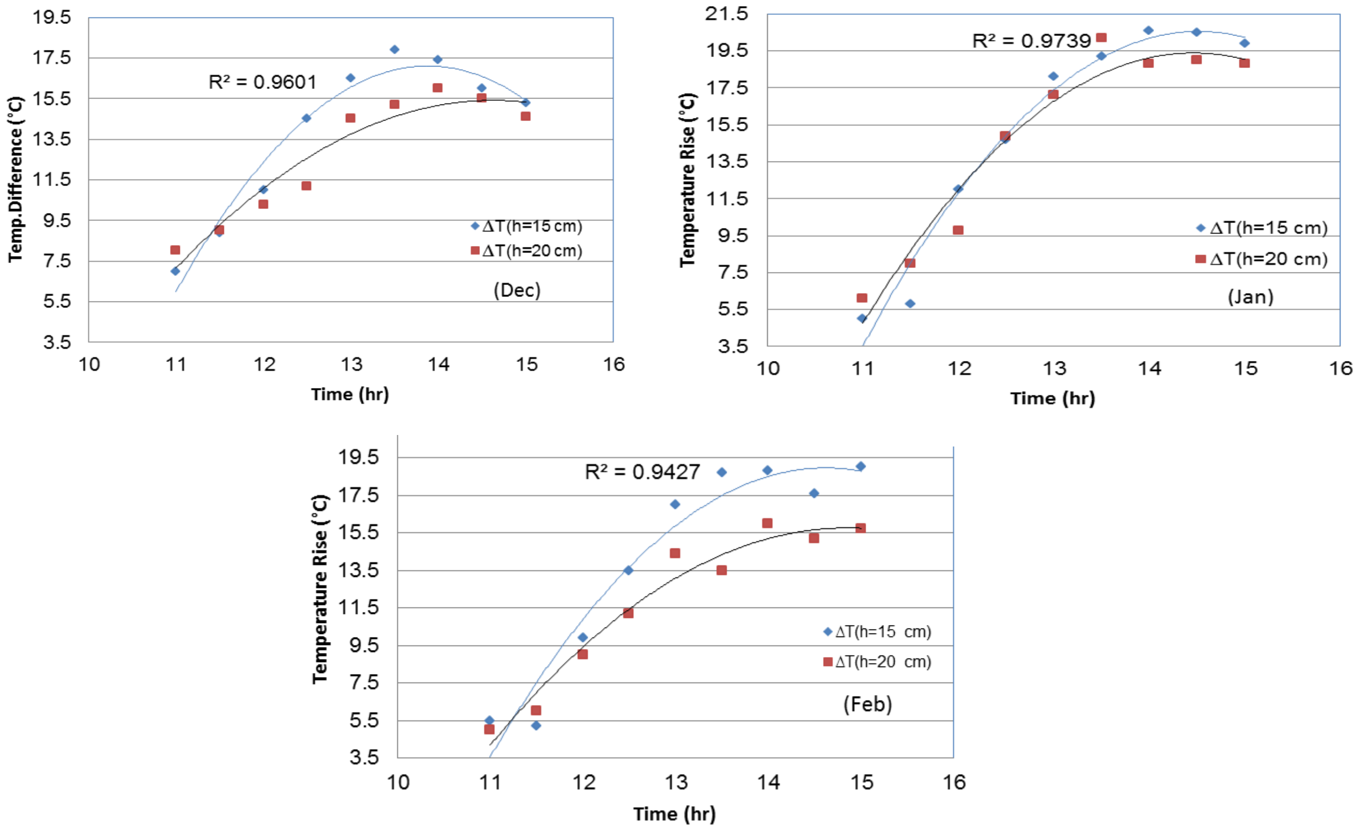

Figure 12. Effect of height on variation of temperature difference with time.

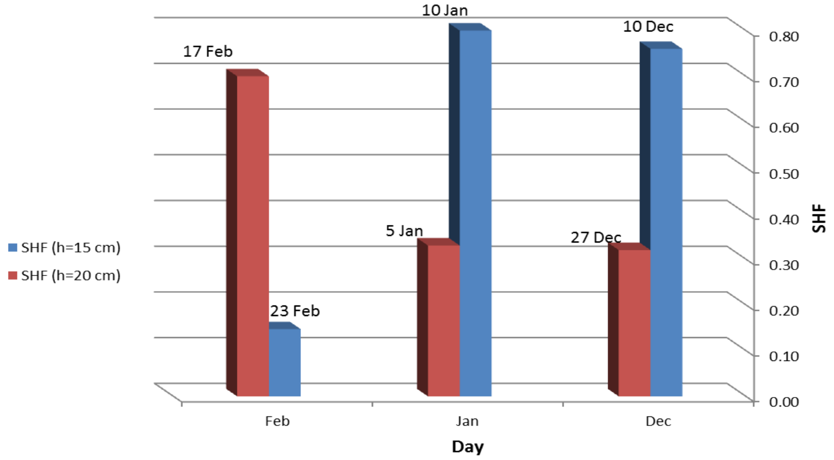

Figure 13. Variation of solar heating fraction for different height of pebble bed (p=0.29, m'=0.018 kg/s).

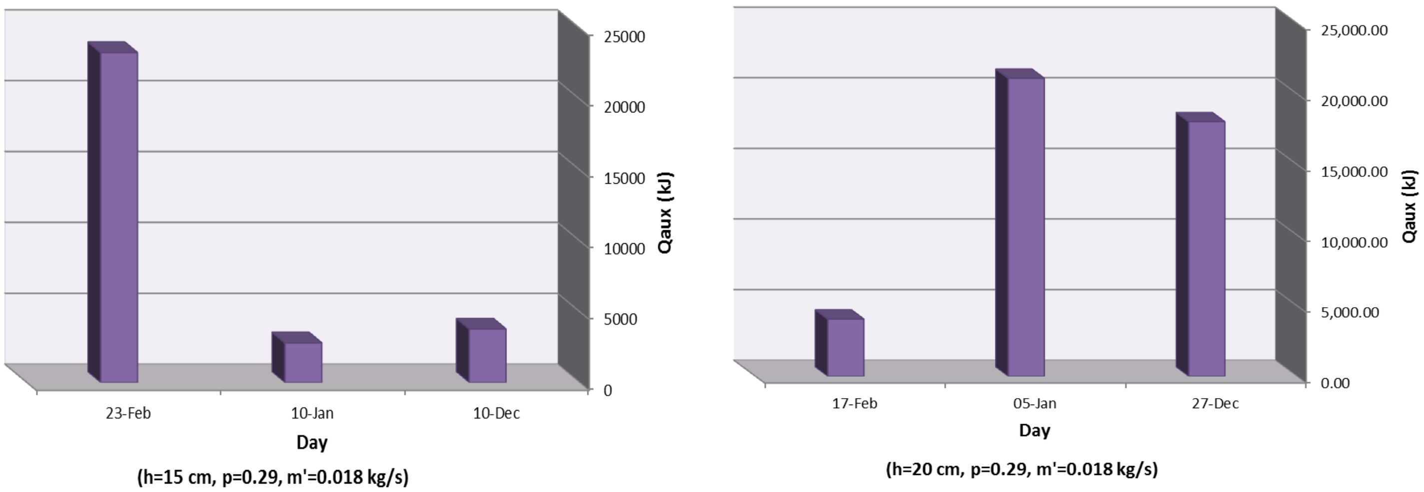

Figure 14. Variation of the auxiliary energy.